

Destruction of the small Fermi surfaces in Na_xCoO_2 by Na disorderD. J. Singh¹ and Deepa Kasinathan²¹Materials Science and Technology Division, Oak Ridge National Laboratory, Oak Ridge, TN 37831-6032 and²Department of Physics, University of California Davis, Davis, CA 95616

(Dated: May 4, 2021)

We show using density functional calculations that the small e_g^0 Fermi surfaces in Na_xCoO_2 are destroyed by Na disorder. This provides a means to resolve the prediction of these sections in band structure calculations with their non-observation in angle resolved photoemission experiments.

PACS numbers:

The layered oxide, Na_xCoO_2 , has attracted considerable interest because of its enhanced thermoelectric properties,¹ and because, when hydrated the material becomes a superconductor, possibly with unconventional pairing.^{2,3} Na_xCoO_2 consists of triangular sheets of Co ions, with nominal d electron count, $5+x$. These are coordinated by distorted edge sharing octahedra, made from triangular sheets of O ions above and below the Co sheets. These CoO_2 tri-layers are stacked in an alternating fashion to form prismatic sites, which contain the Na.

Establishing the electronic structure is requisite for understanding of both the thermoelectric behavior and the superconductivity. Local density approximation (LDA) band structure calculations,^{4,5} show a Fermi level that lies near the top of a narrow manifold of t_{2g} bands, which is separated by a gap from the higher lying e_g derived states. With the actual rhombohedral Co site symmetry, the three t_{2g} orbitals are further divided into an a_g and two degenerate e_g symmetry orbitals, denoted e_g^0 to distinguish them from the higher lying e_g manifold defined by the primary crystal field splitting. Significantly, local density approximation band structure calculations show the presence of two sheets of Fermi surface over a wide range of x . These are a large a_g derived hole cylinder around Γ and six small hole sections along the hexagonal

$-K$ lines. The calculated Fermi surfaces of the hydrated superconducting compound similarly show both a_g and small e_g^0 sections.⁶ While these e_g^0 sections are small, and therefore are not expected to contribute substantially to the conduction, they contribute strongly to the density of states and should be very important for scattering, magnetic susceptibility and other properties because of the two dimensional nature of the material and their heavy mass.^{7,8}

In contrast to the band structure calculations, angle resolved photoemission (ARPES) experiments by several groups at various doping levels observe the large a_g cylinder but do not find the small e_g^0 sections.^{9,10,11,12,13} Early on,⁴ it was noted that although metallic, Na_xCoO_2 had a small band width compared to plausible values for the on-site Coulomb repulsion, U . One explanation that has been advanced for the absence of the e_g^0 sections is that they are destroyed by correlation effects. LDA+U calculations, which incorporate Coulomb repulsion in a static mean field like way, have indeed shown

that the small sections are removed for reasonable values of U .^{7,14} However, the LDA+U approximation also favors insulating, charge ordered ground states.⁷ Removal of the small sections is also found in the large U limit Gutzwiller approximation.¹⁵ However, in metals, fluctuations, including charge and orbital fluctuations are favored by kinetic energy considerations and the presence of e_g^0 sections would open more degrees of freedom for fluctuations. Dynamical mean field calculations, which incorporate physics like the LDA+U approximation, but in a beyond mean field manner that incorporates fluctuations, yielded the opposite tendency to the LDA+U approximation, i.e. an enlargement of the e_g^0 pockets over the LDA.¹⁶ Low temperature specific heat measurements on superconducting hydrated Na_xCoO_2 show two distinct energy gaps,¹⁷ which is difficult to understand if there is only one, simple Fermi surface. Thus, the discrepancy between the ARPES and LDA Fermi surfaces remains a puzzle. Here we resolve this puzzle by showing that the small sections are destroyed by scattering due to the Na disorder inherent in the structural chemistry of Na_xCoO_2 .

As mentioned, the Na ions are contained in O prisms defined by the O triangular lattice. There are two types of sites: Those directly above a Co ion, denoted Na_{c_o} here, and those above the holes in the Co sheet, denoted Na_{h} (these are directly above the O atoms in the O layer on the opposite side of the Co sheet). There is one Na_{c_o} and one Na_{h} site per Co, with a total Na filling of x per Co, or $x=2$ per site. However, the number of available sites is smaller since occupation of an Na_{c_o} next to an occupied Na_{h} site or vice versa would be highly unfavorable due to the short Na-Na distance of 1.64 Å that would result. In fact, local structures that within a given Na layer have Na of a given type (Na_{c_o} or Na_{h}) having Na neighbors of the same type are favored. Also Na in adjacent layers tend not to coordinate the same Co ion.^{18,19,20}

To investigate the effect of Na ion ordering, we focus on the $x=2/3$ composition and perform electronic structure calculations for two supercells with different Na orderings and Co sites. Specifically, we report results for two $\sqrt{3}\times\sqrt{3}$ cells with lattice parameters $a=2.84\text{Å}$, $c=10.81\text{Å}$. Results are reported for the ideal structure, with apical O height $z_o=0.0864$ (Ref. 5), but with different Na orderings, and for fully relaxed atomic positions. Each

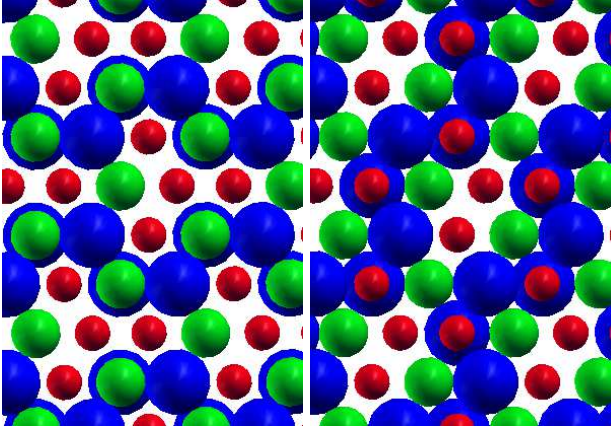


FIG. 1: (color online) Structure of two supercells, A (left) and B (right). Na ions are indicated by the large blue spheres, Co by the mid-size green spheres, and O by the small red spheres.

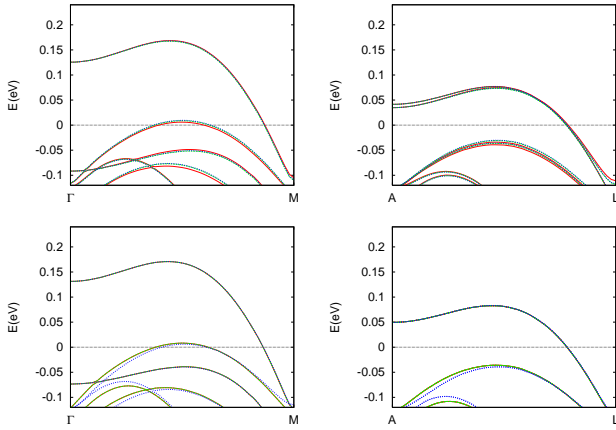


FIG. 2: (color online) Band dispersions along the $-M$ and $A-L$ directions for the two relaxed supercells: A (top) and B (bottom). The different line types are for the three $-M$ or $A-L$ directions, separated by 120° , which are non-equivalent in the relaxed supercells.

supercell contains 6 Co and 12 Na sites in two layers. The two supercells, as shown in Fig. 1 are: (A) with one Na layer on the Na_{c_o} sites and the other on the Na_{a_h} sites (both with two Na atoms per layer); and (B) with both Na layers on the Na_{a_h} sites.

The calculations were done within the local density approximation with the general potential linearized augmented plane wave (LAPW) method including local orbitals.^{21,22,23} Well converged basis sets, of approximately 2600 LAPW functions plus local orbitals, were used, with LAPW sphere radii of $1.96 a_0$ for the Na and Co and $1.52 a_0$ for O.

The calculated band structures near the Fermi energy, E_F , for the relaxed cells are shown in Fig. 2, along the supercell $-M$ lines. Due to the $\sqrt{3} \times \sqrt{3}$ supercell periodicity, these are folded $-K$ directions in the original hexagonal zone, and therefore intersect the small pocket-

ets. The band structures obtained for the two supercells are very similar to each other and to the virtual crystal band structure.⁵ In particular, at this doping level there is sufficient k_z dispersion that only the outer of the two a_g and e_g^0 pairs of bands produce Fermi surfaces in the $k_z = 0$ plane, while both a_g and neither e_g^0 bands produce Fermi surfaces at $k_z = 1=2$. This differs in detail from virtual crystal calculations,⁵ where both e_g^0 bands reach a maximum above E_F in the $k_z = 1=2$ plane. This difference in the e_g^0 , but not the a_g topology, when using real Na ions instead of the virtual crystal approximation is an indication that variations in the Na potential due to disorder could localize the e_g^0 carriers. In any case, the maximum of the a_g band is 0.17 eV above E_F , while the e_g^0 maximum is only 0.01 eV above E_F . Besides the positions of the band maxima, there is also a large difference in band velocity along the $-M$ line, $v(a_g) = 1.4$ eV \AA^{-1} , $v(e_g^0) = 0.3$ eV \AA^{-1} .

The second indication of localization of the e_g^0 carriers comes from the Co and O 1s core level positions. These measure the variation of the local electrostatic potential in the supercells. Supercell A has two different types of Co, the four Co coordinated by a Na in the prism immediately above or below and the two without. In the unrelaxed cell those with Na are 0.033 eV higher than the Co without. This variation is higher than the energy difference between the e_g^0 band maximum and E_F . Secondly, while supercell B has all Co equivalently coordinated, the O sites differ in coordination in both supercells. The variation in O core level position is 0.06 eV in both A and B. This variation may be significant because the bands are in fact hybridized Co-O bands. The variations in core level position are largely preserved in the relaxed cells, and structural inhomogeneities in the Co-O bond lengths and angles are introduced, which will also contribute to scattering. The variation of Co 1s levels is reduced to 0.029 eV in supercell A, i.e. only slightly smaller than in the unrelaxed cell, and still larger than the e_g^0 band maximum relative to E_F , while the variation in the O 1s positions increases to 0.07 eV.²⁵ Thus the potential variations due to Na disorder are strong enough to localize the e_g states.²⁶

The relaxation in supercell A is larger than in supercell B. This is because the Co and nearby Na_{c_o} ions are both positive and move apart by 0.02 \AA , while the nearest neighbor Na-O distance contracts by between 0.006 \AA to 0.01 \AA , depending on the site. There are also distortions of the O cages. Measured by the difference between the shortest and longest Co-O distance for a given Co site, these range from 0.01 \AA ($2/3$ of the Co in B) to 0.015 \AA (for the Co with Na_{c_o} neighbors in A).

In any case, the results show that scattering due to Na disorder is strong enough to localize the e_g^0 carriers at $x = 2=3$. The actual position of the e_g^0 band maximum relative to E_F is a function of doping, as is the Na distribution. The linear size of the e_g^0 Fermi surface, as predicted by band structure calculations varies from zero at high x to approximately 0.18% of the dimension of the

zone at $x = 0.3$.^{5,8} At $x = 0.3$, the e_g^0 maximum lies 0.1 eV above E_F . Observation of this Fermi surface would require a mean free path for e_g^0 carriers of at least the inverse of this reciprocal space size. At $x = 0.3$ this would imply $\lambda_{eg^0} > 50 \text{ \AA}$, where λ_{eg^0} is the mean free path for the heavy carriers on the small Fermi surfaces. In metals with Fermi surfaces having similar orbital character (here $\text{Co } t_{2g}$), the constant scattering time approximation is reasonable. Then $\lambda = v_F \tau$, where τ is a scattering time, v_F is the Fermi velocity on a given section of Fermi surface and λ is the mean free path for carriers on that section. Taking the ratio of the velocities for the two sheets along the Γ -M line, the implication is that a mean free path $\lambda_{ag} \approx 250 \text{ \AA}$, for the main Fermi surface would be needed in order for the small section to be seen. Note that the small sections are elliptical in shape, elongated along Γ -M, so the criterion in the tangential direction would be the same as the velocity is larger, and the size smaller, in proportion. Within kinetic transport theory, the conductivity is given by $\sigma = e^2 N(E_F) v_F^2 \tau$, where $N(E_F)$ is the density of states at E_F and v_F is the average Fermi velocity in the direction in which the conductivity is measured. Thus the large difference in the Fermi velocity between the large and small sections means that the conductivity is dominated by the large section, regardless of whether the small sections are present or not. Thus the measured resistivity is, for practical purposes, governed by the transport in the a_g section. Depending on the doping level, Na_xCoO_2 samples of the type used in photoemission have been reported to have ratios of the resistivity at 300K to the residual resistivity in the range of 20 - 30,^{1,27} and resistivity saturation at or below 600K. These values are inconsistent with a mean free path at low temperature as long as 250 \AA. We note that although the small sections become larger as x is lowered, they do so more slowly than in a rigid band picture and the large ratio of the v_F on the two surfaces is

maintained.^{5,8}

Very recent high resolution photoemission work¹¹ shows dispersions of the a_g and e_g^0 bands below E_F that have a noticeable anti-crossing along Γ -K, for which the one electron e_g^0 and a_g bands have different symmetries and would not mix. The observed mixing is strong. Furthermore, a non-dispersive spectral weight is seen just below E_F in the region where the e_g^0 band is above E_F in band calculations. Both of these features are natural if scattering strong enough to localize the e_g^0 pockets is assumed.

To summarize we find that disorder in the Na layer of Na_xCoO_2 produces sufficiently strong potential variations to localize the e_g^0 Fermi surface pockets at least for high x . Other scattering mechanisms and defects will enhance this tendency. We argue that the non-observation of the small pockets and other features seen in recent photoemission experiments can be qualitatively understood within this framework, specifically that the carriers associated with the small pocket are localized due to scattering related to Na and other disorder. In the hydrated superconducting compound, each Na is coordinated with four H_2O molecules, is far from the CoO_2 sheets and the Na is in a more ordered pattern with respect to the Co atoms. One may speculate that this leads to a sufficient reduction in the potential scattering due to the Na, and that this could lead to the re-appearance of the e_g^0 sections.

We are grateful for helpful discussions with H. Ding, M. Z. Hasan, D. Mandrus, R. Jin, I.I. Mazin, M. D. Johannes and W. E. Pickett. Research at ORNL sponsored by the Division of Materials Sciences and Engineering, Office of Basic Energy Sciences, U.S. Department of Energy, under contract DE-AC05-00OR22725 with Oak Ridge National Laboratory, managed and operated by UT-Battelle, LLC. Work at UC Davis supported by DOE grant DE-FG03-01ER45876.

-
- ¹ I. Terasaki, Y. Sasago and K. Uchinokura, *Phys. Rev. B* 56, 12685 (1997).
 - ² K. Takada, H. Sakurai, E. Takayama-Muromachi, F. Izumi, R. A. Dilanian and T. Sasaki, *Nature* 422, 53 (2003).
 - ³ I.I. Mazin and M. D. Johannes, *Nature Physics* 1, 91 (2005).
 - ⁴ D. J. Singh, *Phys. Rev. B* 61, 13397 (2000).
 - ⁵ M. D. Johannes, D. A. Papaconstantopoulos, D. J. Singh and M. J. Mehl, *Europhys. Lett.* 68, 433 (2004).
 - ⁶ M. D. Johannes and D. J. Singh, *Phys. Rev. B* 70, 014507 (2004).
 - ⁷ K. W. Lee, J. Kunes and W. E. Pickett, *Phys. Rev. B* 70, 045104 (2004).
 - ⁸ M. D. Johannes, I.I. Mazin, D. J. Singh and D. A. Papaconstantopoulos, *Phys. Rev. Lett.* 93, 097005 (2004).
 - ⁹ M. Z. Hasan, Y. D. Chuang, D. Qian, Y. W. Li, Y. K. Ong, A. K. Upurin, A. V. Fedorov, R. K. Kimmberling, E. Rotenberg, K. Rossnagel, Z. Hussain, H. Koh, N. S. Rogado, M. L. Foo and R. J. Cava, *Phys. Rev. Lett.* 92, 246402 (2004).
 - ¹⁰ H. B. Yang, S. C. Wang, A. K. P. Sekharan, H. Matsui, S. Souma, T. Sato, T. Takahashi, T. Takeuchi, J. C. Cam-puzano, R. Jin, B. C. Sales, D. Mandrus, Z. Wang and H. Ding, *Phys. Rev. Lett.* 92, 246403 (2004).
 - ¹¹ H. B. Yang, Z. H. Pan, A. K. P. Sekharan, T. Sato, S. Souma, T. Takahashi, R. Jin, B. C. Sales, D. Mandrus, A. V. Fedorov, Z. Wang and H. Ding, *Phys. Rev. Lett.* 95, 146401 (2005).
 - ¹² D. Qian, L. Wray, D. Hsieh, D. Wu, J. L. Luo, N. L. Wang, A. K. Upurin, A. Fedorov, R. J. Cava, L. Vicini and M. Z. Hasan, *Phys. Rev. Lett.* 96, 046407 (2006).
 - ¹³ M. Z. Hasan, D. Qian, Y. Li, A. V. Fedorov, Y. D. Chuang, A. P. K. Upurin, M. L. Foo and R. J. Cava, *cond-mat/0501530* (2005).
 - ¹⁴ P. Zhang, W. Luo, M. L. Cohen and S. G. Louie, *Phys. Rev. Lett.* 93, 236402 (2004).
 - ¹⁵ S. Zhou, M. Gao, H. Ding, P. A. Lee and Z. Wang, *Phys. Rev. Lett.* 94, 206401 (2005).
 - ¹⁶ H. Ishida, M. D. Johannes and A. Liebsch, *Phys. Rev. Lett.*

- 94, 196401 (2005).
- ¹⁷ N. Oeschler, R.A. Fisher, N.E. Phillips, J.E. Gordon, M.L. Foo and R.J. Cava, *Physica B* 359, 479 (2005); cond-mat/0503690 (2005).
- ¹⁸ H.W. Zandbergen, M. Foo, Q. Xu, V. Kumar and R.J. Cava, *Phys. Rev. B* 70, 024101 (2004).
- ¹⁹ P. Zhang, R.B. Capaz, M.L. Cohen and S.G. Louie, *Phys. Rev. B* 71, 153102 (2005).
- ²⁰ Q. Huang, M.L. Foo, R.A. Pascal, Jr., J.W. Lynn, B.H. Toby, T. He, H.W. Zandbergen and R.J. Cava, *Phys. Rev. B* 70, 184110 (2004).
- ²¹ D.J. Singh and L. Nordstrom, *Plane waves, Pseudopotentials and the LAPW Method*, 2nd Ed. (Springer, Berlin, 2006).
- ²² D. Singh, *Phys. Rev. B* 43, 6388 (1991).
- ²³ Calculations were done using the WIEN2K code,²⁴ and an independent code. These were cross-checked by calculations of the core level positions using independent choices of parameters.
- ²⁴ P. Blaha, K. Schwarz, G.K.H. Madsen, D. Kvasnicka, and J. Luitz, *WIEN2K*, 2002, an Augmented Plane Wave + Local Orbitals Program for calculating crystal properties (Karlheinz Schwarz, Technische Universität Wien, Austria).
- ²⁵ This trend of increased O variation and decreased Co variation in the relaxed structure reflects the electrostatic repulsion between Co and Na, which causes them to move apart, and the attraction between O and Na, which causes some O ions to move closer to Na; Y.S. Meng, A. Van der Ven, M.K.Y. Chan and G. Ceder, *Phys. Rev. B* 72, 172103 (2005).
- ²⁶ P.A. Lee and T.V. Ramakrishnan, *Rev. Mod. Phys.* 57, 287 (1985).
- ²⁷ Y. Wang, N.S. Rogado, R.J. Cava and N.P. Ong, *Nature* 423, 425 (2003).